ELSEVIER

Chemical Engineering Journal 141 (2008) 242–249

Chemical Engineering Journal

www.elsevier.com/locate/cej

Enhancement of mass transfer performance of liquid–liquid system by droplet flow in microchannels

J.H. Xu, J. Tan, S.W. Li, G.S. Luo *

The State Key Lab of Chemical Engineering, Department of Chemical Engineering, Tsinghua University, Beijing 100084, China

Received 6 July 2007; received in revised form 11 December 2007; accepted 28 December 2007

Abstract

Two multiphase flow microfluidic devices based on the use of droplet flow to enhance the mass transfer performance have been specially developed. Mass transfer performance data has been obtained by monitoring the extraction of succinic acid from *n*-butanol to aqueous drops containing NaOH. Monodisperse aqueous droplets with average diameters of 130–550 μm were generated, and the mass transfer time was 0.4–4.0 s accordingly. The mass transfer rate was 10–1000 times higher comparing to the traditional liquid–liquid systems. Vortex flow patterns within the droplet were generated during droplet forming stage that enhanced mass transfer rate greatly. The mass transfer during droplet formation stage contributed at least 30% of the total mass transfer quantities from the theoretical analyzing. And the mass transfer coefficients were 10–100 times higher than that of droplet moving stage. These results were very different to the mass transfer in conventional extraction processes. The mass transfer mechanism during droplet forming stage in microscale should be investigated fundamentally in the further work. The mass transfer results from this study indicate that droplet flow within a microscale environment offers a viable alternative for two-phase reaction or separation systems.
© 2008 Elsevier B.V. All rights reserved.

Keywords: Monodisperse droplet; Mass transfer; Microchannels

1. Introduction

The use of microfluidics offers a number of advantages over conventional flow control technology [1–3]. High surface-to-volume ratio and small volume expedite the chemical reaction in microfluidic devices and improve the product yield. A high-efficiency way for mass transfer and reaction enhancement is by segmented flow in microchannels or capillaries. Vortex flow patterns generated by the shearing motion within fluid segments enhances mixing within segments and improves mass transfer across the interface [4–6]. Micro-segments can be applied in modular synthetic chemistry, quantitative chemical analyses and synthesis of colloidal nanoparticles [7–9].

Recently, attention has been paid to immiscible liquid–liquid systems at microscale with a focus on intensification of mass transfer and reactions by dispersing one phase into the other as droplets in micro-meters. Droplet flow in microchannels offers potentially further improvement in mass transfer. The time to equilibrium scales with the diffusive path length squared. Therefore, if a droplet of radius 300 μm is created, the time to equilibrium would be expected to decrease about 100-fold compared to a 3 mm droplet. Novel micromixers have been developed using the microchannel dispersion method by Benz and Pennemann et al. [10,11]. They found that efficiency as much as 95% could be reached in short time with the droplet diameters from 20 to 150 μm in a liquid–liquid extraction process. In the same period, our research group developed another kind of micro-structured mixer based on the membrane emulsification technology [12–14]. The results showed that in microscale dispersion extraction processes the mass transfer efficiency could be as much as 100%, and the mass transfer time was less than 0.5 s. Droplet flow in microscale has been also applied for liquid–liquid micro-extraction, nanoparticle synthesis, rapid reaction processes, and so on [15–17].

In the present work, we attempt to investigate the interfacial mass transfer and reaction performance of liquid–liquid dispersed system by using droplet flow in microchannels. The effects of two phase flow rates and two phase concentrations on droplet size and mass transfer process have been studied. And the mass transfer rate was compared with that of conventional extraction processes. Finally, the mass transfer mechanisms were discussed.

* Corresponding author. Tel.: +86 10 62783870; fax: +86 10 62783870.
E-mail address: gsluo@tsinghua.edu.cn (G.S. Luo).

1385-8947/$ – see front matter © 2008 Elsevier B.V. All rights reserved.
doi:10.1016/j.cej.2007.12.030

2. Experimental

2.1. Microfluidic devices

The experiments were performed in two types of microfluidic devices fabricated on 100 mm × 20 mm × 5 mm polymethyl metacrylate (PMMA) plates using an end mill. In the co-flowing device, the continuous and dispersed phase flow channels dimensions are approximately 100 μm wide × 100 μm high. The measured channel dimensions were approximately 560 μm wide × 500 μm high (Fig. 1a). In the flow-focusing device, the continuous and dispersed phase flow channels dimensions are approximately 150 μm wide × 100 μm high. The measured channel dimensions were approximately 300 μm wide × 250 μm high (Fig. 1b). Two microsyringe pumps and three gastight microsyringes were used to pump the two phases into the microfluidic devices, respectively.

2.2. Materials

A simple acid-base reaction was used as the basis of this study because, being extremely rapid, its progress is controlled by the diffusion of the reactants within the two phases. It has the further advantage that conventional pH indicators can be used to follow the reaction progress. These also clarify the photographic distinction between the two phases. Methyl Phenol Red pH indicator was added to distilled water to create a saturated system, which was filtered and then diluted to by a factor of two with more distilled water. This was then used to produce aqueous solution of NaOH in the range from 0.1 to 0.3 mol/L. *n*-Butanol was used as the organic phase. Succinic acid was added into *n*-butanol to produce organic solutions of 0.138 and 0.23 mol/L. Because the PMMA plate is hydrophobic, so the organic phase was used as the continuous phase and the aqueous phase was used as the dispersed phase. The solubility of NaOH in the organic phase is negligible whereas succinic acid is completely soluble in the aqueous phase. The reaction is then assumed to take place solely in the aqueous phase as succinic acid diffuses across the interface. The reaction involved in this work is given in Eq. (1). This requires a half mole of succinic acid per mole NaOH:

$$\mathrm{HOOC(CH_2)_2COOH} + 2\mathrm{NaOH} \rightarrow \mathrm{NaOOC(CH_2)_2COONa} + 2\mathrm{H_2O} \quad (1)$$

2.3. Visualization and analysis

Experiments were carried out with a microscope at the magnification of 100×. A high-speed CCD video camera was connected to the microscope and the images were recorded with a frequency of 200 images per second. The diameter of aqueous drops generated was measured from microscope images. Colour change was observed within the aqueous droplets as succinic acid diffused into the aqueous phase reacting with NaOH and changing the pH of the droplet.

Analysis of the titration within the microfluidic device was performed through measurements of the distance along the channel at which the pH indicator in the aqueous phase changed from violet red to yellow. Since the pH indicator changed colour as the local pH passed through 7.2, this change indicated that the amount of succinic acid which transferred into the aqueous drop was about half of NaOH present within the drop. From this data the time requirement for the transfer of a given proportion of succinic acid from the organic phase to the aqueous phase could be obtained.

The droplets sizes and distances required to achieve a complete colour change within the aqueous droplets for all the experiments were recorded and analyzed. Then the average droplets diameters (d_{av}), time requirements for droplet formation (t_F), and time requirements for acid transfer during moving stage (t_m) could be obtained in different experimental conditions. And the mass transfer time, which means the total time requirements for mass transfer, could be calculated as the sum of t_F and t_m. For each condition, we repeated the experiment for three times, the standard deviations of the measured average droplets diameters (d_{av}) and time requirements for acid transfer during moving stage (t_m) were both less than 10%.

3. Results and discussion

3.1. Typical micrographs during mass transfer processes

Fig. 2 shows the typical micrographs of colour change within the droplet during droplet forming stage at the cross-junction and moving in the measured channel separately in both of the microfluidic devices. Vortex flow patterns within the aqueous droplet could be observed during droplet forming stage from Fig. 2a. The vortex was mainly generated by the shearing motion of the continuous phase, and it enhanced mixing within the

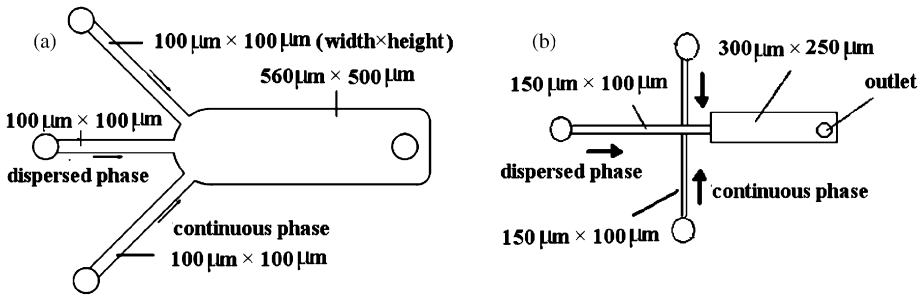

Fig. 1. The microfluidic devices: (a) co-flowing device; (b) flow-focusing device.

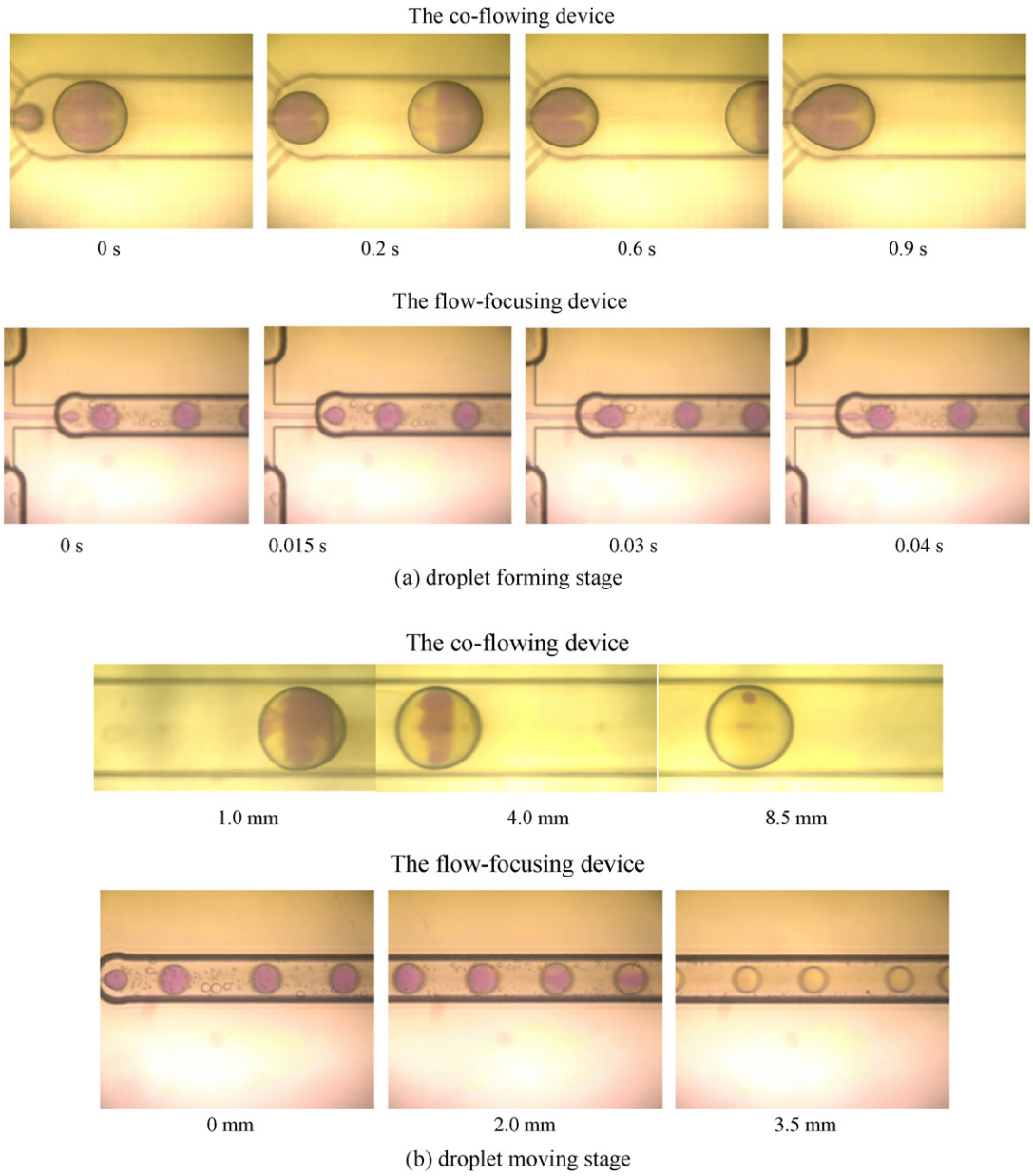

Fig. 2. Typical micrographs of colour change within the droplet during mass transfer processes. The experimental conditions are, aqueous phase concentration $C_{NaOH} = 0.10$ mol/L, organic phase concentration $C_{acid} = 0.138$ mol/L; organic phase flow rate $Q_o = 20$ μL/min, and aqueous phase flow rate $Q_w = 5$ μL/min.

droplet. While during droplet moving stage, there was almost no relative-moving between two phases because of the co-flowing of continuous organic phase and aqueous phase. And the mass transfer process could be treated as the mass transfer of succinic acid at the interface of stagnant droplet in the quiescent continuous phase.

3.2. *Effects of two phase flow rates on droplet size and time required for acid transfer*

Firstly, we investigated the influences of two phase flow velocities on the droplet size and mass transfer time. Fig. 3 shows the effects of total flow velocity on the calculated average droplet diameter and mass transfer time at three fixed flow ratios of the two phases in the co-flowing device. The average droplet diameter was observed to decrease with the increase of total flow velocity, while increased with the increase of phase ratio (Q_w/Q_o). These results were similar to that of without mass transfer. On the other hand, the mass transfer time decreased as total flow velocity was increased, while increased with the increase of phase ratio (Q_w/Q_o). The results can be explained by the differences in droplet size which affected the mass transfer rate. It also can be seen that mass transfer time decreased from 3.0 to 2.0 s with the average droplet diameter from 550 to 380 μm.

Fig. 4 shows the effects of total flow velocity on the average droplet diameter and mass transfer time in the flow-focusing device. It can be seen that mass transfer time decreased from 0.8

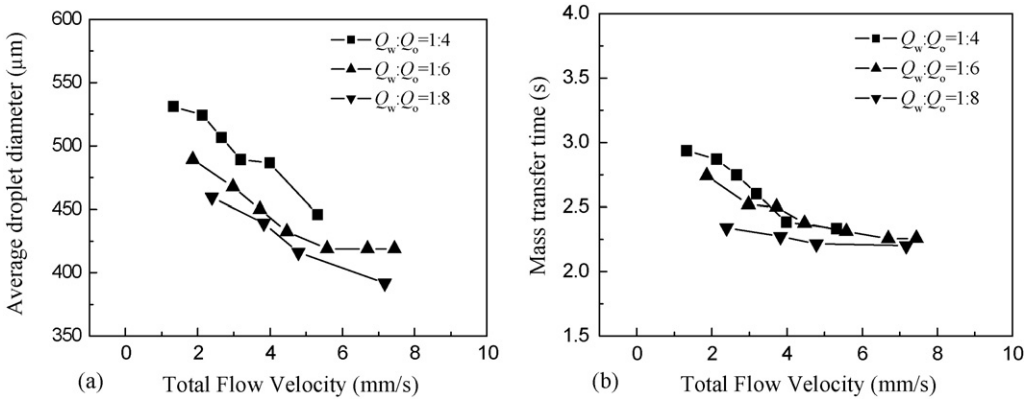

Fig. 3. Effects of two phase flow velocities on the average droplet diameter and mass transfer time in the co-flowing device. C_{NaOH} = 0.1 mol/L, C_{acid} = 0.138 mol/L.

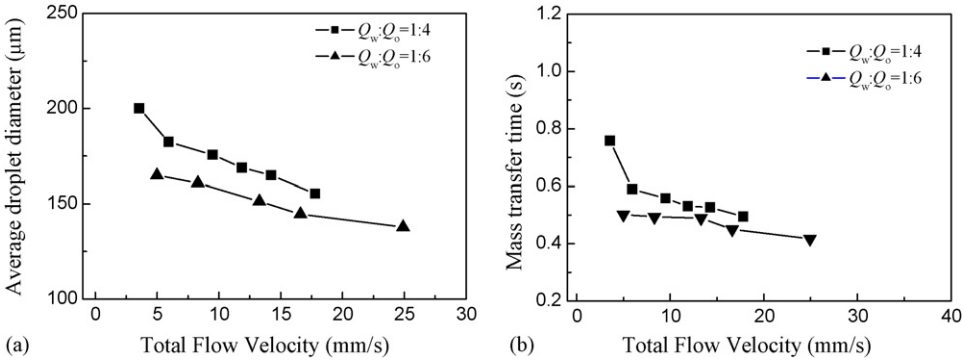

Fig. 4. Effects of two phase flow velocities on the average droplet diameter and mass transfer time in the flow-focusing device. C_{NaOH} = 0.1 mol/L, C_{acid} = 0.138 mol/L.

to 0.4 s with the average droplet diameter from 200 to 130 μm. And the mass transfer rate increased about 10 times by reducing the droplet size from 550 to 130 μm.

3.3. Effects of two phase concentrations

Fig. 5 shows the effect of total flow velocity on the average droplet diameter and mass transfer time at different fixed NaOH concentrations in the co-flowing device. It can be seen from Fig. 4a that the average droplet diameter increased with the increase of NaOH concentration at fixed two phase flow velocities. Reasons of the difference in droplet size may lie in the influence of chemical composition on systems' interfacial tension. The mass transfer time also increased as the NaOH concentration was increased, which was mainly caused by the increase of droplet diameter and the proportion of succinic acid required to change the indicator colour. Fig. 6 shows the effects of total flow velocity on the average droplet diameter and mass transfer time at different fixed succinic acid concentrations. The average droplet diameter also increased with the increases of acid concentration at fixed two phase flow velocities. While the mass transfer time decreased as the succinic acid concentration was increased. The mainly reason lies in that the mass transfer rate increases with the increase of acid concentration.

In the flow-focusing device, the variations of droplet size and mass transfer time with two phase concentrations were found to

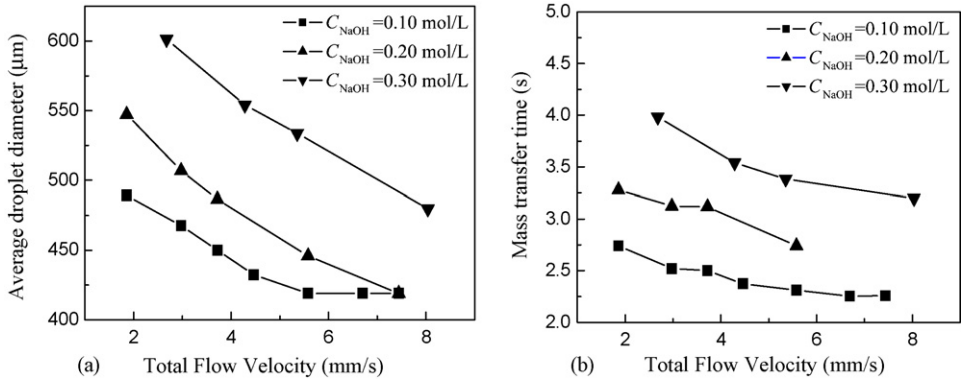

Fig. 5. Effect of the NaOH concentration on the average droplet diameter and mass transfer time in the co-flowing device. C_{acid} = 0.138 mol/L, Q_w:Q_o = 1:6.

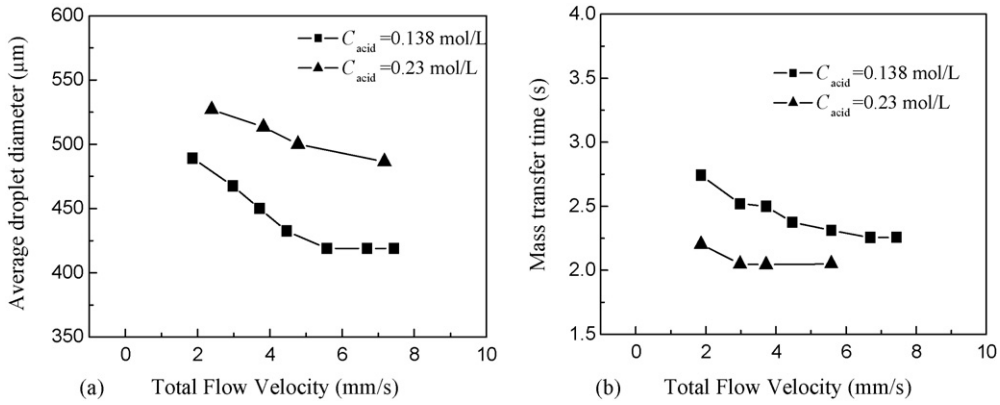

Fig. 6. Effect of the succinic acid concentration on the average droplet diameter and mass transfer time in the co-flowing device. C_{NaOH} = 0.10 mol/L, Q_w:Q_o = 1:6.

be similar to that in the co-flowing device. Because of the smaller channel size, the formed droplet diameter was in the range of 150–250 μm, and the mass transfer time was at 0.5–1.5 s.

3.4. Enhancement of mass transfer process

A more formal comparison of the mass transfer performance of the droplet flow in microscale with other systems may be achieved through an estimation of the volumetric mass transfer coefficient. In general terms the transfer rate of succinic acid between the droplets can be written as follows:

$$\frac{dC}{dt} = K_c a \Delta C \quad (2)$$

where ΔC is the concentration differential between the organic and aqueous phase. The interfacial area per unit volume across which the transfer takes place is represented by a, and the mass transfer coefficient for the system by K_c. For the model reaction, which is the neutralization of succinic acid, the intrinsic kinetics is extremely fast. Therefore it was assumed that succinic acid was consumed almost instantaneously as it entered the aqueous droplets which contained an excess of NaOH. The concentration differential between the droplets was therefore assumed to be

$$\Delta C = C_{ORG} - C_{AQ} \approx C_{ORG} \quad (3)$$

Combining the approximation given in Eq. (3) with Eq. (2) yields the following equation for the rate of consumption of the acid

$$\frac{dC_{ORG}}{dt} = -K_c a C_{ORG} \quad (4)$$

From Eq. (4) the time required for the proportion α of succinic acid to be consumed in the titration should be given by

$$t = -\frac{1}{K_c a}\ln(1-\alpha) \quad (5)$$

From Eq. (5), the estimation of the product of mass transfer coefficient and interfacial area per unit volume, which means the volumetric mass transfer coefficient $K_c a$, could be provided from the following equation:

$$K_c a = -\frac{1}{t}\ln(1-\alpha) \quad (6)$$

Values of $K_c a$ were obtained from the experimental data using Eq. (6). Table 1 shows the comparison of volumetric mass transfer coefficient between the droplet flow in microchannels and that in the conventional extraction columns. It is found that the mass transfer rate was increased with the decrease of formed droplet diameter. In the co-flowing microchannels, the value of $K_c a$ was about 0.1 s^{-1} when the droplet diameter was 0.35 mm, which was around 100 times higher to that in the extraction columns with the droplet diameter 3.0 mm. While in the flow-focusing microchannels, the volumetric mass transfer coefficient could be increased to 0.5 s^{-1} with the droplet diameter decreased to 0.13 mm. The increase of mass transfer rate was mainly caused by the enhancement of mass transfer during droplet forming and moving stages in microscale. During droplet moving stage, the mass transfer coefficient and interfacial area per unit volume both increase with the decrease of droplet diameter, and the mass transfer rate increases greatly. During droplet forming stage, vortex flow patterns within the aqueous droplet generated by the shearing motion of continuous phase could also enhance the mass transfer process. So we should consider the contribution of mass transfer enhancement at both droplet moving and forming stages.

3.5. Discussion of mass transfer contributions during droplet forming and moving stages

During droplet moving stage, there was no relative-moving velocity between two phases because of the co-flowing of continuous organic phase and aqueous drops. So we could assume the mass transfer during droplet moving stage as the mass transfer of succinic acid at the interface of stagnant droplet in the quiescent continuous phase, and the mass transfer fraction during droplet moving stage will be calculated. Then we can quanti-

Table 1
Comparison of $K_c a$ and average droplet diameter d_{av} between droplet flow in microscale and conventional extraction processes

Mass transfer process	d_{av} (mm)	$K_c a$ (s^{-1})
Droplet flow in co-flowing microchannels	0.35–0.55	0.02–0.1
Droplet flow in flow-focusing microchannels	0.13–0.25	0.23–0.5
Conventional extraction columns [18,19]	2.0–3.0	10^{-4}–10^{-3}

tatively confirm the mass transfer contribution during droplet moving stage. It would be usable for us to develop the mass transfer mechanism during droplet forming stage in microscale.

The mass transfer coefficients inside and outside a stagnant droplet in the quiescent continuous phase could be calculated as [20,21]

$$Sh_d = \frac{k_d d}{D_d} = 6.58 \tag{7}$$

$$Sh_c = \frac{k_c d}{D_c} = 2.0 + 0.76 Re^{1/2} Sc^{1/3} \tag{8}$$

From Eqs. (7) and (8), the total mass transfer coefficient K_c can be predicted as

$$\frac{1}{K_c} = \frac{1}{k_c} + \frac{1}{m k_d} \tag{9}$$

where $m = c_d^*/c_c = 0.935$, is the distribution coefficient of succinic acid between two phases. From Eq. (9), the values of K_c in our experiments were in the range of 3.3–5.7 $\times 10^{-6}$ m/s during droplet moving stage. From the mass transfer Eq. (10),

$$N = K_c A(c_c - c_{ci}) \tag{10}$$

where c_{ci} equals zero in our experiments, c_c is the main concentration of succinic acid in the continuous phase. Based on the mass conservation equation,

$$K_c A(c_c - c_{ci})\,dt = -V_c\,dc_c \tag{11}$$

$$\int_0^t K_c A\,dt = -V_c \int_{c_0'}^{c} \frac{1}{c_c - c_{ci}}\,dc_c = -V_c \ln\left(\frac{c_c - c_{ci}}{c_0' - c_{ci}}\right) \tag{12}$$

where $V_c = (Q_c/Q_d)V_d$, and $r = (Q_c/Q_d)$, is the flow ratio of two phases. The following equation is obtained by simplifying Eqs. (11) and (12),

$$\ln\left(\frac{c_0'}{c_t}\right) = \frac{6tK_c}{r d_d} \tag{13}$$

herein, d_d is the droplet diameter. So the initial concentration of the acid during droplet moving stage can be calculated from Eq. (13). We define a parameter y, which means the mass transfer contribution fraction of droplet forming stage, as the following equation:

$$y = \frac{c_0 - c_0'}{c_0 - c_t} \tag{14}$$

Then, the contribution of mass transfer during droplet forming stage to the total mass transfer process could be obtained from Eq. (14). It can be seen from Fig. 7 that the mass transfer during droplet forming stage contributed at least 30% of the total mass transfer quantities in our experiments. So the contribution of mass transfer during droplet forming stage cannot be neglected at droplet flow in microchannels. While in the conventional extraction process, the contribution of mass transfer during droplet forming stage is usually less than 10%. The difference is mainly because of the size effect in microscale.

3.6. Estimation of mass transfer coefficients during droplet forming stage

The mass transfer coefficients during droplet forming stage could also be calculated from the mass conservation equation (11). The difference is that the mass transfer area A is depended on the droplet forming time. And the relationship between the droplet diameter and forming time can be obtained be the following equation at fixed dispersed flow rate Q_d

$$d = \left(\frac{6Q_d}{\pi} t\right)^{1/3} \tag{15}$$

Substituting d from Eq. (15) into Eq. (11),

$$K_{cf} t^{-(1/3)}\,dt = -\left(\frac{6Q_d}{\pi}\right)^{1/3} \frac{r}{6} \frac{dc_c}{c_c} \tag{16}$$

From Eq. (16), the average mass transfer coefficient during droplet forming stage is,

$$K_{cf} = \frac{(6Q_d/\pi)^{1/3} r \ln(c_0/c_0')}{9 t_f^{2/3}} = \frac{d_d r \ln(c_0/c_0')}{9 t_f} \tag{17}$$

where t_f is the time needed for droplet forming. Values of the average mass transfer coefficient K_{cf} were obtained from the experimental date using Eq. (17), which can be seen in Fig. 8.

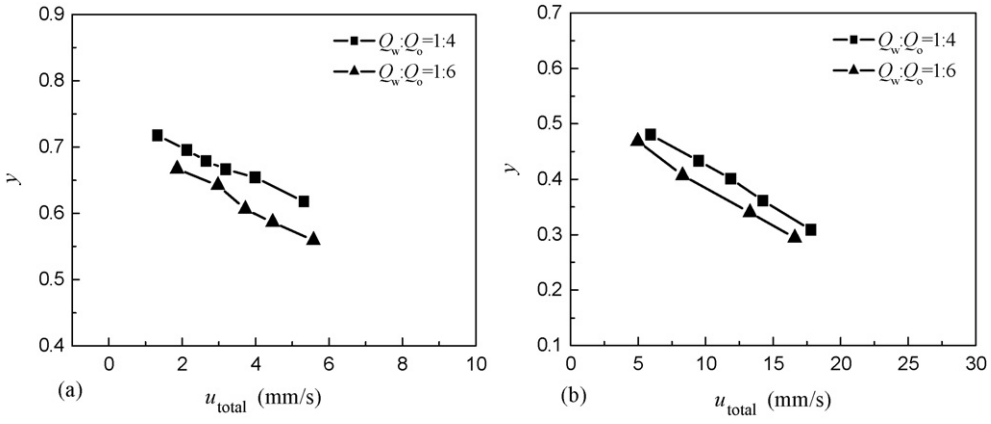

Fig. 7. The mass transfer contribution fraction during droplet forming stage: (a) co-flowing device; (b) flow-focusing device.

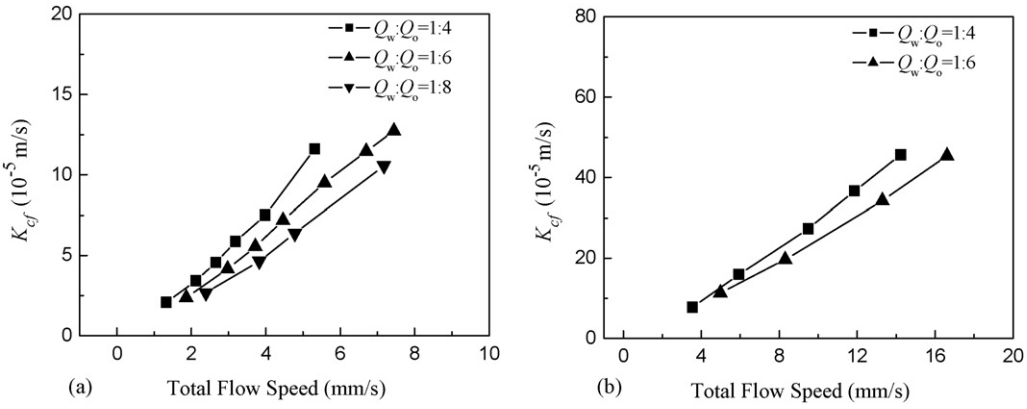

Fig. 8. Mass transfer coefficients during drop forming stage K_{cf}. C_{NaOH} = 0.1 mol/L, C_{acid} = 0.138 mol/L: (a) co-flowing device; (b) flow-focusing device.

These are found to be in the range of 2.0–50.0 × 10^{-5} m/s, with higher values being obtained for the higher flow velocities and lower droplet diameter. And the mass transfer coefficients were around 10–100 times higher than that of droplet moving stage. The mainly reason was that vortex flow patterns within the oil droplet generated by the shearing motion of the continuous phase enhances mass transfer and reaction rate during droplet forming stage. And it facilitates the mass transfer performance greatly. These results were very different to the mass transfer in conventional extraction processes. The mass transfer mechanism during droplet forming stage in microscale should be investigated fundamentally in the further work.

4. Conclusions

In this work, we investigated the enhancement of mass transfer performance of liquid–liquid dispersed system in microscale by droplet flow in two types of microchannels. Mass transfer time decreased from 4.0 to 0.4 s with the average droplet diameter from 550 to 130 μm. Mass transfer rates were 10–1000 times higher compared with that of the conventional extraction processes. Based on the qualitative analysis, mass transfer occurred both at droplet forming and moving stages. There was almost no relative-moving velocity between two phases because of the co-flowing of continuous organic phase and aqueous phase during droplet moving stage. While during droplet forming stage, vortex flow patterns within the droplet could enhance mass transfer process. And the mass transfer coefficients increased at 1–2 stages compared to that of droplet moving stage. The mass transfer during droplet formation stage contributed at least 30% of the total mass transfer quantities from the theoretical analyzing. Our results indicate that droplet flow within a microscale environment offers a viable alternative for two-phase reaction or mass transfer systems. The mass transfer mechanism during droplet forming stage in microscale should be investigated fundamentally in the further work.

Acknowledgments

We gratefully acknowledge the supports of the National Natural Science Foundation of China (20476050, 20490200, 20525622) and SRFDP (20040003032) on this work.

References

[1] P.A. Auroux, D. Iossifidis, D.R. Reyes, A. Manz, Micro total analysis systems. 2. Analytical standard operations and applications, Anal. Chem. 74 (2002) 2637–2652.
[2] K. Jensen, A.P. Lee, The science & applications of droplets in microfluidic devices, Lab Chip 4 (2004) 31N–32N.
[3] M. Tokeshi, T. Minagawa, T. Kitamori, Integration of a microextraction system on a glass chip: ion-pair solvent extraction of Fe(II) with 4,7-diphenyl-1,10-phenanthrolinedisulfonic acid and tri-*n*-octylmethylammonium chloride, Anal. Chem. 72 (2000) 1711–1714.
[4] J.R. Burns, C. Ramshaw, The intensification of rapid reactions in multiphase systems using slug flow in capillaries, Lab Chip 1 (2001) 10–15.
[5] M. Ueno, H. Hisamoto, T. Kitamori, S. Kobayashi, Phase-transfer alkylation reactions using microreactors, Chem. Commun. 7 (2003) 936–937.
[6] N. Harries, J.R. Burns, D.A. Barrow, C. Ramshaw, A numerical model for segmented flow in a microreactor, Int. J. Heat Mass Transfer 46 (2003) 3313–3322.
[7] J.M. Köhler, Th. Henkel, A. Grodrian, Digital reaction technology by micro segmented flow—components, concepts and applications, Chem. Eng. J. 101 (2004) 201–216.
[8] B. Zheng, J.D. Tice, R.F. Ismagilov, Formation of droplets of alternating composition in microfluidic channels and applications to indexing of concentrations in droplet-based assays, Anal. Chem. 76 (2004) 4977–4982.
[9] S.A. Khan, A. Gunther, M.A. Schemidt, K.F. Jensen, Microfluidic synthesis of colloidal silica, Langmuir 20 (2004) 8604–8611.
[10] K. Benz, K.P. Jäckel, K.J. Regenauer, J. Schiewe, K. Drese, W. Ehrfeld, V. Hessel, H. Lowe, Utilization of micromixers for extraction processes, Chem. Eng. Technol. 24 (2001) 11–17.
[11] H. Pennemann, S. Hardt, V. Hessel, P. Lob, F. Weise, Micromixer based liquid/liquid dispersion, Chem. Eng. Technol. 28 (2005) 501–508.
[12] G.G. Chen, G.S. Luo, Y. Sun, J.H. Xu, J.D. Wang, A ceramic microfiltration tube membrane dispersion extractor, AIChE J. 50 (2004) 382–387.
[13] J.H. Xu, G.S. Luo, G.G. Chen, B. Tan, Mass transfer performance and two-phase flow characteristic in membrane dispersion mini-extractor, J. Membr. Sci. 249 (2005) 75–81.
[14] G.G. Chen, G.S. Luo, S.W. Li, J.H. Xu, Experimental approaches to understanding of a micro-structure device, AIChE J. 51 (2005) 2923–2929.
[15] J.G. Kraji, M.A. Schemidt, K.F. Jensen, Surfactant-enhanced liquid–liquid extraction in microfluidic channels with inline electric-field enhanced coalescence, Lab Chip 5 (2005) 531–535.

[16] T. Yanagishita, Y. Tomabechi, K. Nishio, H. Masuda, Preparation of monodisperse SiO_2 nanoparticles by membrane emulsification using ideally ordered anodic porous alumin, Langmuir 20 (2004) 554–555.
[17] L. Hung, K.M. Choi, W. Tseng, Y. Tan, K.J. Shea, A.P. Lee, Alternating droplet generation and controlled dynamic droplet fusion in microfluidic device for CdS nanoparticle synthesis, Lab Chip 6 (2006) 174–178.
[18] G.S. Luo, H.B. Li, W.Y. Fei, J.D. Wang, A general correlation of mass transfer in extraction columns, Chin. J. Chem. Eng. 6 (1998) 233–238.
[19] G.S. Luo, H.B. Li, W.Y. Fei, J.D. Wang, A simplified correlation of mass transfer in plused sieve plate extraction, Chem. Eng. Technol. 21 (1998) 15–19.
[20] R. Kronig, H.C. Brink, On the theory of extraction from falling drop, Appl. Sci. Res. 2 (1950) 42–156.
[21] P.N. Rowe, R.T. Calxton, T.B. Lewis, Heat and mass transfer from a single sphere in an extensive flowing fluid, Trans. Inst. Chem. Eng. 43 (1965) 14–31.